A PAPER ON THE TROPICAL INTRASEASONAL OSCILLATION PUBLISHED IN 1963 IN A CHINESE JOURNAL

Tim Li, Lu Wang, Melinda Peng, Bin Wang, Chidong Zhang, William Lau, and Hung-Chi Kuo

A study published in Chinese in 1963 documented a 40–50-day oscillation in the Asian monsoon region, eight years earlier than its discovery by Madden and Julian in the early 1970s.

Madden and Julian (1971, hereafter MJ71) unveiled a 40–50-day oscillation in the tropospheric zonal wind using radiosonde observation at a single station (i.e., Canton Island) in the central Pacific. This oscillation was later connected to a broad global tropical circulation using observations from multiple stations (Madden and Julian 1972). The intraseasonal signal documented by Madden and Julian is now known as the Madden–Julian oscillation (MJO). These two articles by Madden and Julian are among the most influential studies in modern meteorology. The originally identified MJO signal is confined in the 40–50-day period with zonal wavenumber 1 and eastward-propagating characteristics, which were confirmed by later studies using modern observational data (Weickmann 1983; Murakami and Nakazawa 1985; Lau and Chan 1986). The oscillation was also shown to be of a more broadband pattern (20–90 days) than the original 40–50-day period (e.g., Krishnamurti and Subrahmanyam 1982; Wang and Rui 1990; Hendon and Salby 1994; Annamalai and Slingo 2001; Zhang 2005). Recent theoretical and diagnostic studies indicated that equatorial waves interacting with moisture, convection, and boundary layer dynamics build the fundamental mechanism for the eastward propagation of the MJO (Hsu and Li 2012; Sobel and Maloney 2013; Jiang et al. 2015; Wang et al. 2016; Wang et al. 2017). Initiation of MJO convection

AFFILIATIONS: Li, L. Wang, and B. Wang—Key Laboratory of Meteorological Disaster, Ministry of Education, and Joint International Research Laboratory of Climate and Environmental Change, and Collaborative Innovation Center on Forecast and Evaluation of Meteorological Disasters, Nanjing University of Information Science and Technology, Nanjing, China, and International Pacific Research Center, and Department of Atmospheric Sciences, School of Ocean and Earth Science and Technology, University of Hawai'i at Mānoa, Honolulu, Hawaii; Peng—Naval Research Laboratory, Monterey, California; Zhang—NOAA/Pacific Marine Environmental Laboratory, Seattle, Washington; Lau—Earth System Science Interdisciplinary Center, University of Maryland, College Park, College Park, Maryland; Kuo—National Taiwan University, Taipei City, Taiwan
CORRESPONDING AUTHOR: Dr. Lu Wang, luwang@hawaii.edu

The abstract for this article can be found in this issue, following the table of contents.
DOI:10.1175/BAMS-D-17-0216.1

In final form 7 February 2018

mostly takes place over the western equatorial Indian Ocean (Zhang and Ling 2017) and is caused by anomalous low-level moisture advection (Zhao et al. 2013), warm advection-induced anomalous ascending motion (Li et al. 2015), intraseasonal SST anomalies (Li et al. 2008), and/or extratropical forcing (Hsu et al. 1990; Zhao et al. 2013). Li (2014) provides a comprehensive review on the dynamics of MJO initiation and propagation.

Table 1. Information on the radiosonde stations used in this study.

Station	WMO ID	Location	Lat, lon	NCEP grid point
1	43371	Thiruvananthapuram	(8.48°N, 76.95°E)	(10°N, 77.5°E)
2	48900	Ho Chi Minh	(10.82°N, 106.67°E)	(10°N, 107.5°E)
3	98836	Zamboanga	(6.9°N, 122.07°E)	(7.5°N, 122.5°E)
4	91334	Chuuk	(7.47°N, 151.85°E)	(7.5°N, 152.5°E)
5	91701	Canton Island	(2.77°S, 171.21°W)	(2.5°S, 170°W)

There is pronounced seasonality in MJO intensity (Madden 1986), frequency (Hartmann et al. 1992), and movement (Wang and Rui 1990). In boreal winter, the MJO is dominated by eastward propagation slightly south of the equator, whereas during boreal summer the eastward-propagating mode weakens substantially (Madden 1986, Wang and Rui 1990, Hendon and Salby 1994) as the northward propagation prevails in the Indian monsoon region (Yasunari 1979; Hartmann and Michelsen 1989; Wang and Xie 1997; Jiang et al. 2004) and the northwestward propagation prevails over the western North Pacific (WNP) (Lau and Chan 1986). The MJO was identified in connection to the fluctuation and migration of the Asian summer monsoon (Murakami 1976; Yasunari 1979, 1980, 1981; Fu et al. 2003). The Monsoon Experiment in 1978–79 (Krishnamurti 1985) provided an opportunity to explore further the intraseasonal oscillations involved in the Asian summer monsoon activities.

The MJO has been identified to have far-reaching impacts on many weather- and climate-related phenomena and linkages to tropical waves, tropical cyclone (TC) genesis, diurnal cycles, El Niño–Southern Oscillation (ENSO), and monsoon circulation patterns (Zhang 2013). In particular, relationships between the MJO and TC genesis have attracted special attention. Liebmann et al. (1994) indicate that western North Pacific TCs are twice as likely during convectively active phases of the MJO. Maloney and Hartmann (1998, 2000a,b) suggest that MJO westerlies may set up favorable conditions for TC development by inducing cyclonic low-level vorticity and near-zero vertical wind shear. When MJO 850-hPa wind anomalies are westerly, small-scale eddies grow through barotropic eddy kinetic energy (EKE) conversion from the mean flow, serving as the energy source for TC development (Maloney and Hartmann 2001; Hartmann and Maloney 2001; Hsu et al. 2011). Numerical experiments by Cao et al. (2014) suggested that both circulation and moisture anomalies associated with the MJO affect TC development. In general, all these findings indicate that the MJO can greatly modulate TC activities in most ocean basins. Operational prediction of the MJO has been improved but remains challenging (Vitart 2014; Xiang et al. 2015; Jiang et al. 2015; Wang et al. 2017). The research on the MJO remains very active to date as more attention is being paid to prediction on subseasonal-to-seasonal (S2S) time scales to fill the gap between climate and weather prediction.

It has come to our attention that a study published in 1963 (Xie et al. 1963, hereafter Xie63) in the Chinese journal *Acta Meteorologica Sinica* documented an oscillatory signal of a 1.5-month period using raw radiosonde data from several stations between 70° and 125°E in the Southeast Asian summer monsoon region. Xie63 was mainly devoted to the investigation of the relation between the Southeast Asian flow and the occurrence of typhoons (TCs in the western Pacific). The data covered three years from 1958 to 1960 for the months of June–September. The 40–50-day signal discovered by Xie63 is strikingly strong as revealed by the variation of the zonal wind component at 700 hPa without any filtering. Xie63 identified that the occurrence of TCs was highly correlated with the variation of low-level westerlies at those stations and was often located in the confluence region where the monsoon westerlies meet the easterly trade winds.

Here is the direct quote, with its English translation, of the abstract of Xie63:

> *The relationship between the basic flows of the low latitudes and the occurrence of typhoons was investigated statistically and synoptically by means of recent three-year radiosonde data. It was found that about 80% of typhoons developed in the eastern flank of the tropical confluence zone between the monsoon westerlies and the easterly trade winds. The westerlies are a large-scale and quasi-steady phenomenon. Thus it is probably reasonable to*

be called the "basic flow" while the typhoons are considered as vortices of smaller scale. There is a quite definite relationship between the time, location and frequency of typhoon genesis and the location and strength of the basic flow in the low latitudes. There was a quasi-periodical oscillation of strength and position of the basic zonal flow with a period longer than one month. Such an oscillation might be helpful for the extended-range forecast of initiation and development of typhoons.

Irrespective of the importance of these findings more than 50 years ago, the original paper by Xie63 remains mostly unknown to the international research community, mainly because it was published in Chinese. The purpose of this study is to bring attention to the study by Xie63 and its originality to *BAMS* readers. We analyzed archived radiosonde data for the same three years from 1958 to 1960 to verify the results of Xie63. We also compared the results by Xie63 and MJ71 by using a longer period of data (1958–70) to cover the analysis period of MJ71 (1957–67). The longer period would allow us to make a better comparison of the strength of the intraseasonal signals in Southeast Asia stations found by Xie63 and in Canton Island discovered by MJ71.

This paper is outlined as follows. The next section describes the radiosondes and reanalysis data. The comparison between Xie63 and MJ71 regarding the 40–50-day signals is given next. We follow with a section devoted to the relationship between the MJO and TC genesis as revealed by Xie63. The final section provides a summary and our conclusions.

BIOGRAPHICAL SKETCH OF PROF. YI-BING XIE

Prof. Yi-Bing Xie (or pronounced sometimes as Yi-Ping Hsieh) was born in 1917. He was a graduate student of Prof. C.-G. Rossby and Prof. E. Palman at the University of Chicago in 1945–49 and got his Ph.D. from the University of Chicago in 1949. He returned to China afterward and served as a professor and deputy chair of the Department of Physics at Peking University, Beijing, China, in 1952. He became a professor and chair of the Department of Geophysics in Peking University in 1978 and was elected as an academician to the Chinese Academy of Sciences in 1980. He received the E. Palman Award in 1988. He passed away in Beijing in 1995 from cancer.

RADIOSONDE DATA, REANALYSIS, AND TYPHOON RECORD. The radiosonde data used by Xie63 mainly came from five tropical stations that are roughly evenly distributed from the Indian Ocean to the central Pacific. Their World Meteorological Organization (WMO) identification numbers and

Fig. 1. Locations of the radiosonde stations examined by Xie63. For detailed information about the location and the WMO identification number of each station, readers are referred to Table 1.

geographical locations are listed in Table 1. To provide a geographical perspective of the station locations, we marked each of them on the Google map in Fig. 1. They were simply referred to as stations 1–5 from west to east. Note that station 91701 (or station 5) located on Canton Island and included in one of Xie63's figures was also analyzed by MJ71. The station dataset used in the current study was retrieved from the PANGAEA archive (https://doi.pangaea.de/10.1594/PANGAEA.823608). This dataset merged available collections of upper-air measurements from as far back as 1920s, including Comprehensive Historical Upper-Air Network (CHUAN) and the Integrated Global Radiosonde Archive (IGRA), which were interpolated to standard pressure levels (Ramella Pralungo et al. 2014). As this dataset provides twice-daily observations, we first calculate the daily mean result and then conduct linear interpolation to fill in missing values.

To obtain a more comprehensive picture, the daily three-dimensional wind fields during 1958–70 from the National Centers for Environmental Prediction–National Center for Atmospheric Research (NCEP–NCAR) reanalysis dataset (Kalnay et al. 1996) are also used. The resolution of the reanalysis data is 2.5° × 2.5°. The information on tropical cyclone genesis dates and locations is obtained online (from www.weather.unisys.com/hurricane/).

THE 40–50-DAY SIGNALS DISCOVERED BY XIE63 AND MJ71. Figure 2 is the original Fig. 2 in Xie63, one of their most important figures. It shows time series of zonal wind at 700 hPa at three radiosonde stations (43371, 48900, and 98836, or stations 1–3 in Fig. 1). The data cover from 1 June to the beginning of September for 1958–60. Red arrows were added to highlight the periods of the westerlies. Note that the periodicity of the westerlies as revealed by Xie63 in Fig. 2 was based on the 5-day running mean of raw data without any spectral analysis.

Below is an English translation of a direct quote from Xie63, summarizing their major finding relevant to Fig. 2:

> *The following are the main results derived from Fig. 2:*
>
> *1) There is a consistent phase change of the zonal wind from Station 43371 to Station 98836. When the westerlies intensified in India, they also intensified in Southeast Asia, with a slight temporal delay.*

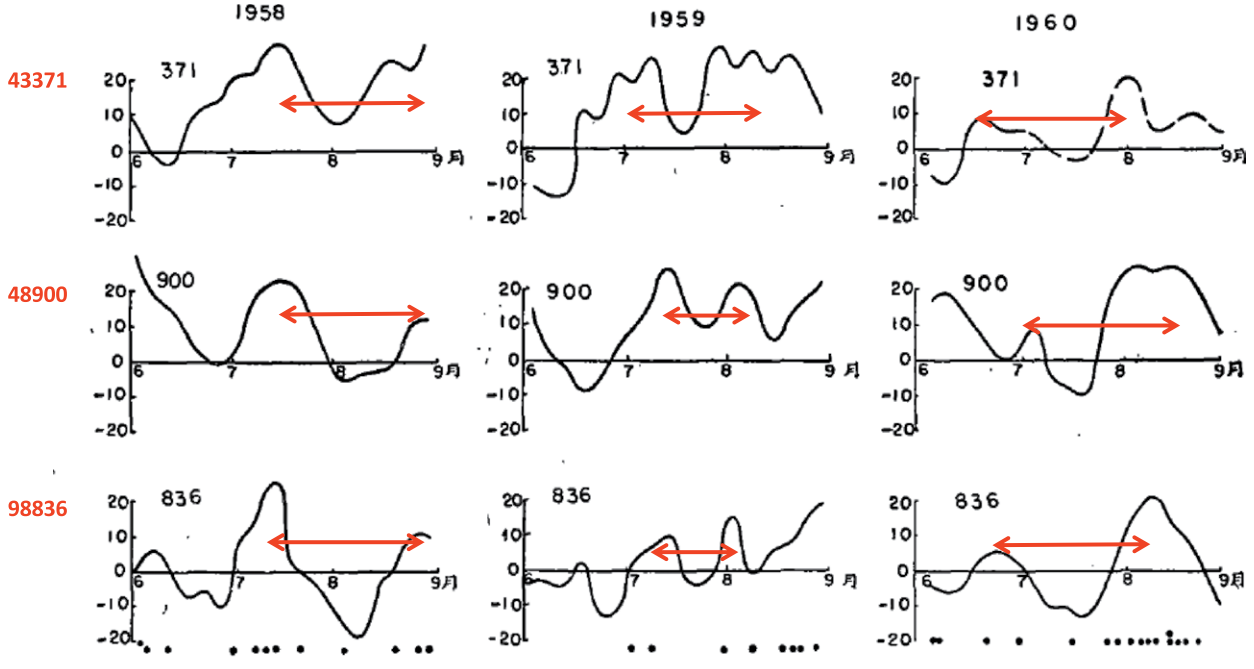

图 2　371，900 和 836 站 700 毫巴五天平均东西向风速与台风发生日期
正值为西风，负值为东风，单位：米/秒，黑点为台风发生日期

FIG. 2. Original Fig. 2 from Xie63 showing time series of 5-day running mean zonal wind (m s^{-1}) at 700 hPa. Positive (negative) values indicate westerlies (easterlies). The abscissa represents the time from 1 Jun to 1 Sep. The station number is marked in each panel and the first column is for 1958, the second for 1959, and the third for 1960. Black dots at the bottom denote the occurrence of typhoons each year. Red arrows are added by the authors of the current study to highlight the intraseasonal periods.

2) Total 36 typhoons occurred during the three summer seasons studied. Among them, 28 typhoons happened when a strong westerly appeared over Southeast Asia (at Stations 48900 and 98836). These typhoons appeared mostly to the eastern flank of a confluence zone between the westerlies and the easterly trade winds. About one fifth of the typhoons occurred when easterlies or weak westerlies appeared over the two stations.

3) The change of zonal wind with time at these stations exhibited a wave like oscillatory characteristic, with an average oscillatory period of around one-and-a-half months. Such an oscillatory feature may benefit for extended-range forecast of typhoon genesis frequency.

To confirm their results, we regenerated the time series of the zonal wind at the same three stations shown in Fig. 2 using the time series of the 5-day running mean zonal wind at 700 hPa based on the radiosonde data (red) and the NCEP–NCAR reanalysis data (black) shown in Fig. 3. The time series based on the NCEP–NCAR reanalysis resembles that of the radiosonde data. Comparing Fig. 3 with Fig. 2 panel by panel indicates that the general patterns are similar with some differences in detail. The difference lies more in the magnitude than in the periodicity. For example, the maxima of the westerlies in the middle of July reach 20 m s^{-1} at station 48836 in Xie63 (bottom-left panel in Fig. 2) while our reproduction (bottom-left panel in Fig. 3) indicates only 10 m s^{-1}, but both of them peak around mid-July. The discrepancies may be simply due to the fact that Fig. 2 in Xie63 was hand drawn. In general, this comparison confirms the low-frequency oscillation in low-level zonal wind with a period longer than 1 month, as explicitly stated by Xie63.

A spectral analysis was conducted on the zonal wind at these stations (see Fig. 4), to further confirm the 1.5-month period indicated by Xie63 by visual inspection. To better compare the strength of the intraseasonal signals at the Southeast Asia stations shown by Xie63 and on Canton Island as discovered by MJ71, a longer analysis period (1958–70) is used. While most analyses in this present study were applied to the zonal wind at 700 hPa following Xie63, 150- and 850-hPa winds were here used to compare directly to MJ71. The original Fig. 2 from MJ71 for station 91701 is included in Fig. 4d for comparison.

The power spectrum analysis reveals significant peaks in MJO variability with a 40–50-day period at all three pressure levels at stations 43371 and 48900. By contrast, at station 91701, the 40–50-day peaks stand out only at 150 and 850 hPa, and they hardly

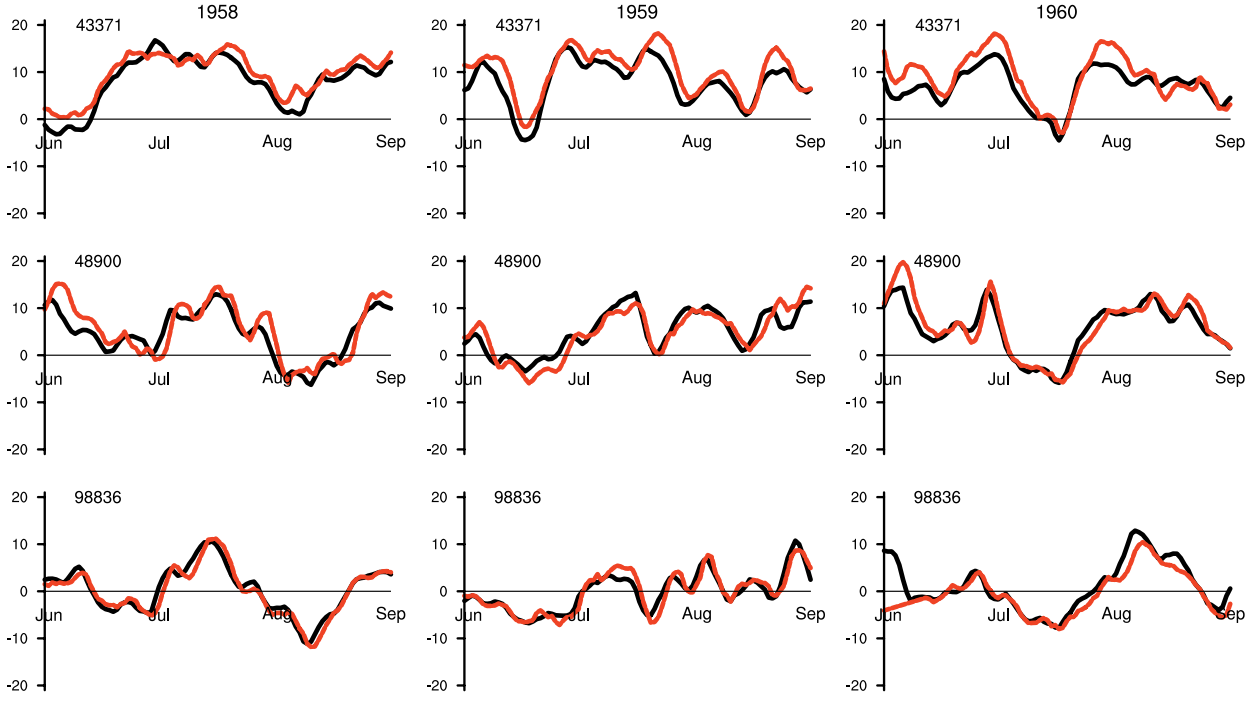

Fig. 3. Time series of 700-hPa 5-day running mean zonal wind (m s^{-1}) from 1 Jun to 1 Sep 1958–60 for the same three stations as in Fig. 2 in Xie63. Red curves are from archived station radiosonde data, and black curves are from nearby NCEP–NCAR gridpoint data.

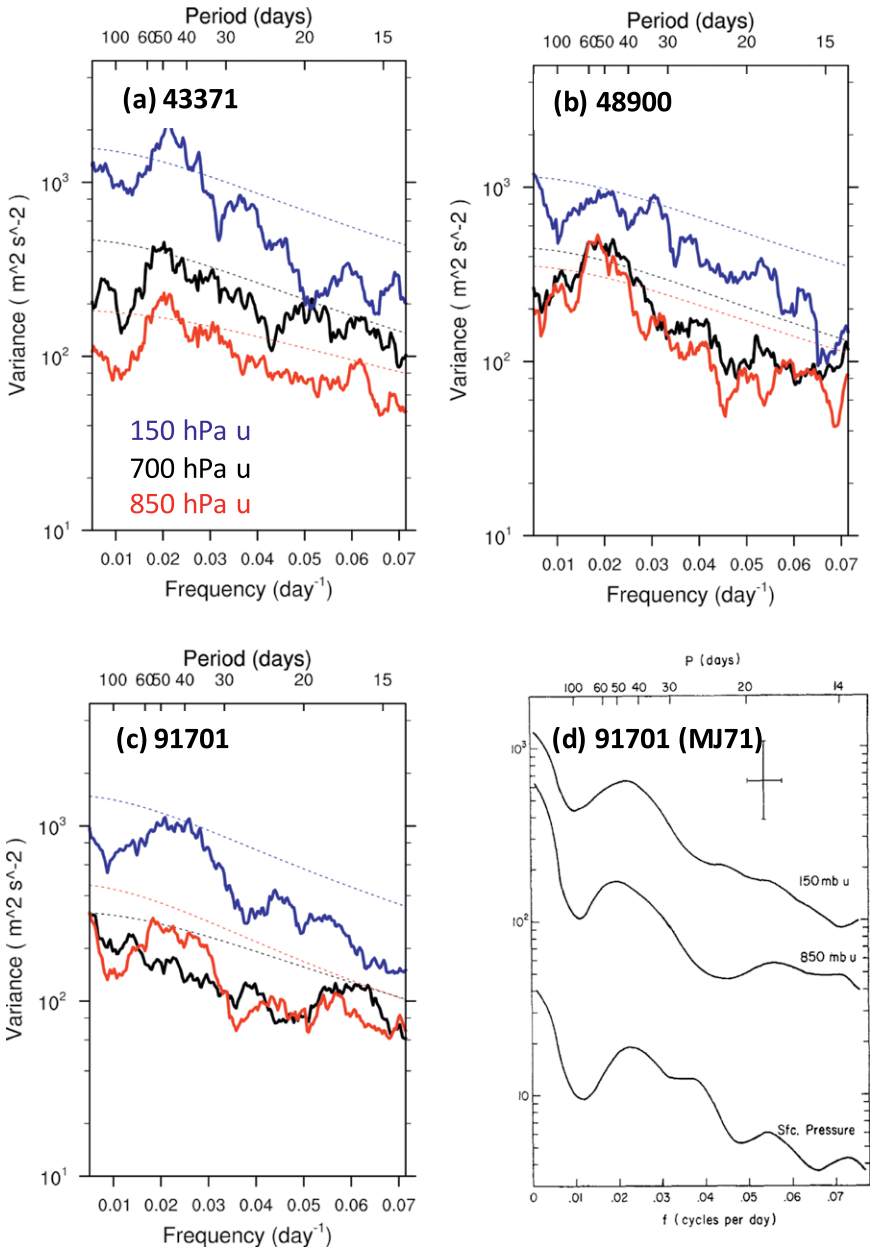

Fig. 4. Variance spectra for the zonal wind (m^2 s^{-2}) at 150 (blue solid), 700 (black solid), and 850 hPa (red solid) for stations (a) 43371, (b) 48900, and (c) 91701 during 1958–70. Dotted lines mark the 95% confidence level. (d) The original Fig. 2 from MJ71 is shown for comparison with the current analysis at station 91701 in (c).

A similar power spectrum analysis result was obtained when only the 3-yr period (1958–60) of data is used. Figure 5 shows the result for comparison with Fig. 4. This would be what Xie63 might have gotten if they had conducted a spectral analysis. The strongest 40–50-day signal appears at station 48900, and this intraseasonal signal is significant at all three pressure levels. At station 43371, the lower-tropospheric 40-day signal is significant, while the upper-tropospheric signal shifts slightly toward a 30-day period.

Then, we calculated the cross spectra between the upper- and lower-level winds at different stations (see Fig. 6) to compare with the original Fig. 1 in MJ71. A positive (negative) coefficient indicates an in-phase (out of phase) relationship between the upper- and lower-level winds. As can be seen, the panels for station 91701 reproduce the original Fig. 1 in MJ71, showing an out-of-phase correlation between the 150- and 850-hPa zonal winds, with the spectra peak in the 40–50-day band. Panels for stations 43371 and 48900 show similar characteristics to those at station 91701.

pass the 95% confidence level. This is consistent with later studies (e.g., Li and Wang 2005) where the maximum MJO variability appears over the Asian–Australian monsoon and warm pool regions. In comparing the results from station 91701 with the original results of MJ71, the power spectrum for longer periods (greater than 100 days) appears weaker in the current analysis than in MJ71. The discrepancy may arise from the different datasets used and the slightly different analysis periods.

To compare zonal wind characteristics from South Asia to the central Pacific, Fig. 7 displays the vertical profile of the zonal wind from 1 June to 30 September 1958 at each station (stations 1–5 marked in Fig. 1) based on radiosonde data. The left panels in Fig. 7 show unfiltered results as in Xie63. Over the South Asia stations west of 125°E (stations 1–3), the periodicity of the westerlies below the 500-hPa level is distinct, and the period of 40–50 days is clear even without filtering. The span of the westerly winds

in time is largest over the Indian Ocean (station 1), decreasing toward the east. The upper levels are all dominated by easterlies. Over the central Pacific (stations 4 and 5), the prevailing wind is mostly easterly throughout the troposphere. The westerly flow at lower levels at station 4 (or 91334) is very weak. As we move to station 5 (or 91701), the westerly wind is barely discernible. The right panels in Fig. 7 display 30–60-day bandpass-filtered signals. A stronger MJO signal appears in the upper troposphere than in the lower troposphere at station 5 (central Pacific), while MJO signals at low levels are as strong as those in the upper level in the monsoon regions (stations 1–3).

Next, we examine the evolutionary patterns of the 700-hPa wind over the summer monsoon region based on NCEP–NCAR reanalysis data during 1958–60. Shown in Fig. 8 are 700-hPa wind and relative vorticity anomalies regressed onto the 700-hPa zonal wind averaged in a reference box enclosing both stations 2 and 3 (green box in Fig. 8). Prior to the regression, all fields were filtered onto a 30–60-day period. Figure 8 displays the lagged regression fields from day −15 to day 0, where day 0 corresponds to a time when the zonal wind anomaly reaches a maximum over the box. At day −15, a pronounced easterly anomaly appears over the reference box, and there is an anomalous cyclone south of it. As time progresses, the northwest–southeast-tilted cyclonic anomaly moves gradually northward. At day 0, local circulation at 10°N is replaced by a pronounced westerly anomaly. The evolution above indicates that the 40–50-day oscillation of the zonal wind examined by Xie63 is a part of the MJO signal in boreal summer with pronounced northward propagation.

The analysis above using archived data reproduced results from Xie63, which pointed out a strong 40–50-day oscillation in the low-level zonal wind in the monsoon regions during boreal summer. The oscillatory signal is so strong that it can be detected by eye without any filtering. These reproduced results confirm that the oscillatory signals documented by Xie63 were real regardless of the short data record used.

RELATION BETWEEN MJO AND TROPICAL CYCLONE GENESIS. Three decades before the studies of Hartmann et al. (1992) and Liebmann et al. (1994), Xie63 pointed out that TC activity in the WNP was modulated by the 40–50-day oscillation of the zonal wind. Figure 2, which is the original Fig. 2 in Xie63, contains the key finding by Xie63 other than those which have been discussed on the periodicity of the zonal wind. The TC occurrence was marked by the small dots at the bottom of the figure for each year of the three years Xie63 investigated. As pointed out by Xie63, about 80% of typhoons in the WNP occurred when strong westerlies appeared at stations 48900 and 98836. To reproduce the results

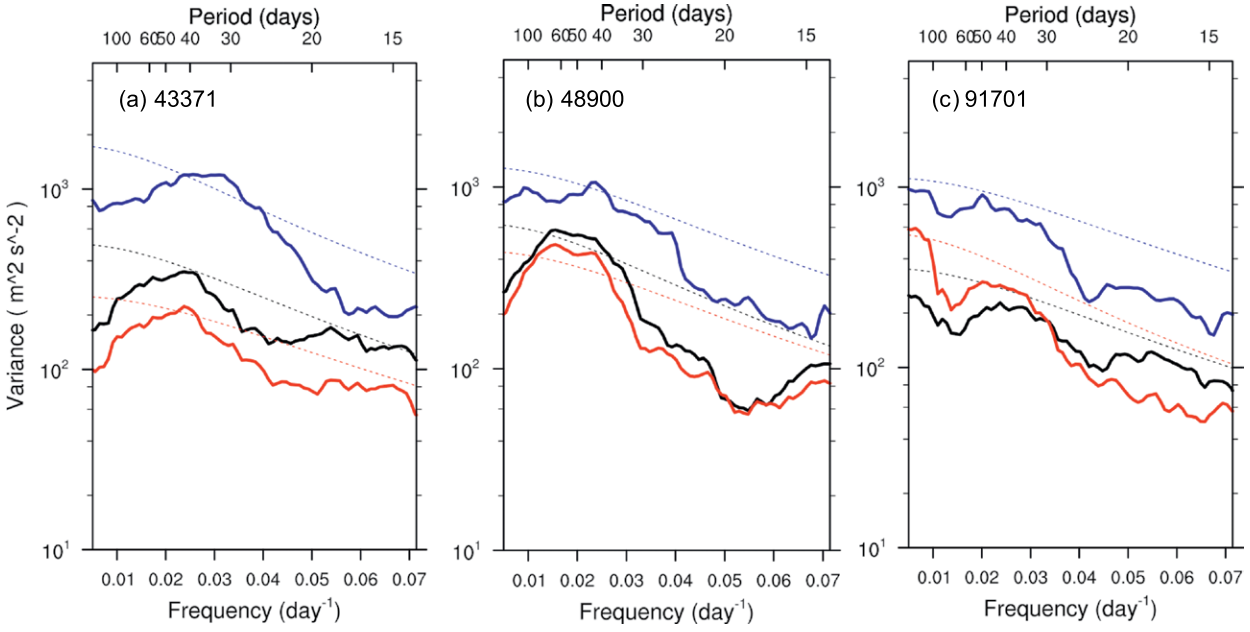

Fig. 5. Variance spectra for zonal wind (m^2 s^{-2}) at 150 (blue solid), 700 (black solid), and 850 hPa (red solid) for stations 43371, 48900, and 91701 during the 3-yr (1958–60) period studied by Xie63. Dotted lines mark the 95% confidence level.

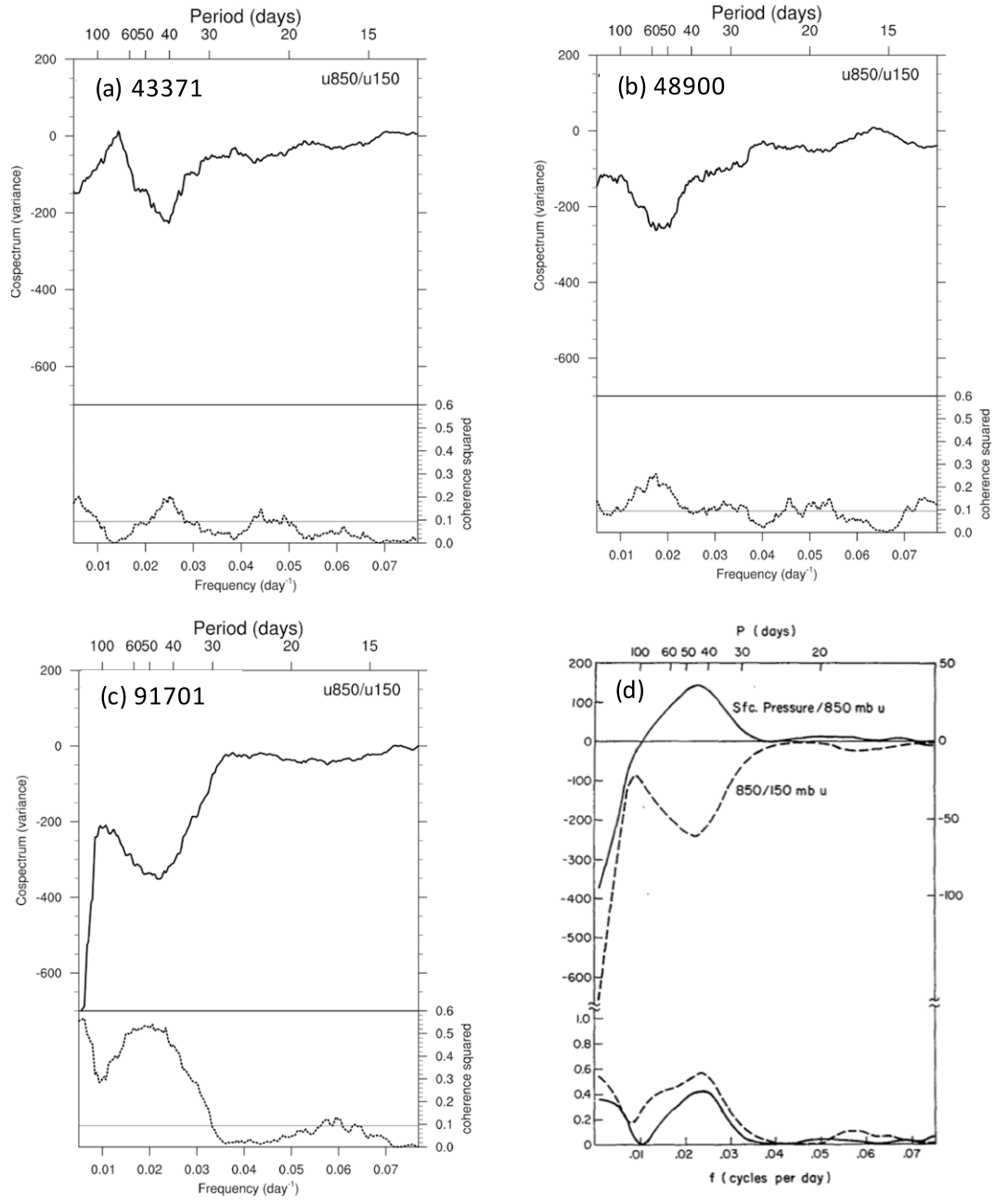

Fig. 6. Cospectrum between 850- and 150-hPa zonal winds ($m^2 s^{-2}$) during 1958–70 (top curves) and coherence-squared statistic for 850- and 150-hPa zonal winds (bottom curves) at stations (a) 43371, (b) 48900, and (c) 91701. The 95% confidence level is denoted by the thin line. (d) The original Fig. 1 from MJ71 is shown for comparison with the current analysis at station 91701 in (c).

in Xie63, we calculated what percentages of TCs in the WNP occurred when the total and anomalous (intraseasonal) zonal wind is westerly at station 48900 during 1958–70, which covers the analysis periods of both Xie63 and MJ71. Out of the total numbers of typhoon occurrences, 92% (60%) of them fell under the total (anomalous) westerly wind period at station 48900. This compares with 80% reported by Xie63 for 1958–60.

Another way to demonstrate the MJO impact is to count the TC genesis number during its westerly and easterly phases. Figures 9a and 9b mark the typhoon genesis locations during the MJO westerly and easterly phases, respectively, which are defined based on the 30–60-day filtered 700-hPa zonal wind anomalies over the reference box of 7.5°–12.5°N, 105°–125°E (denoted by green rectangles). The ratio of TC genesis numbers is about 2:1 between the westerly and

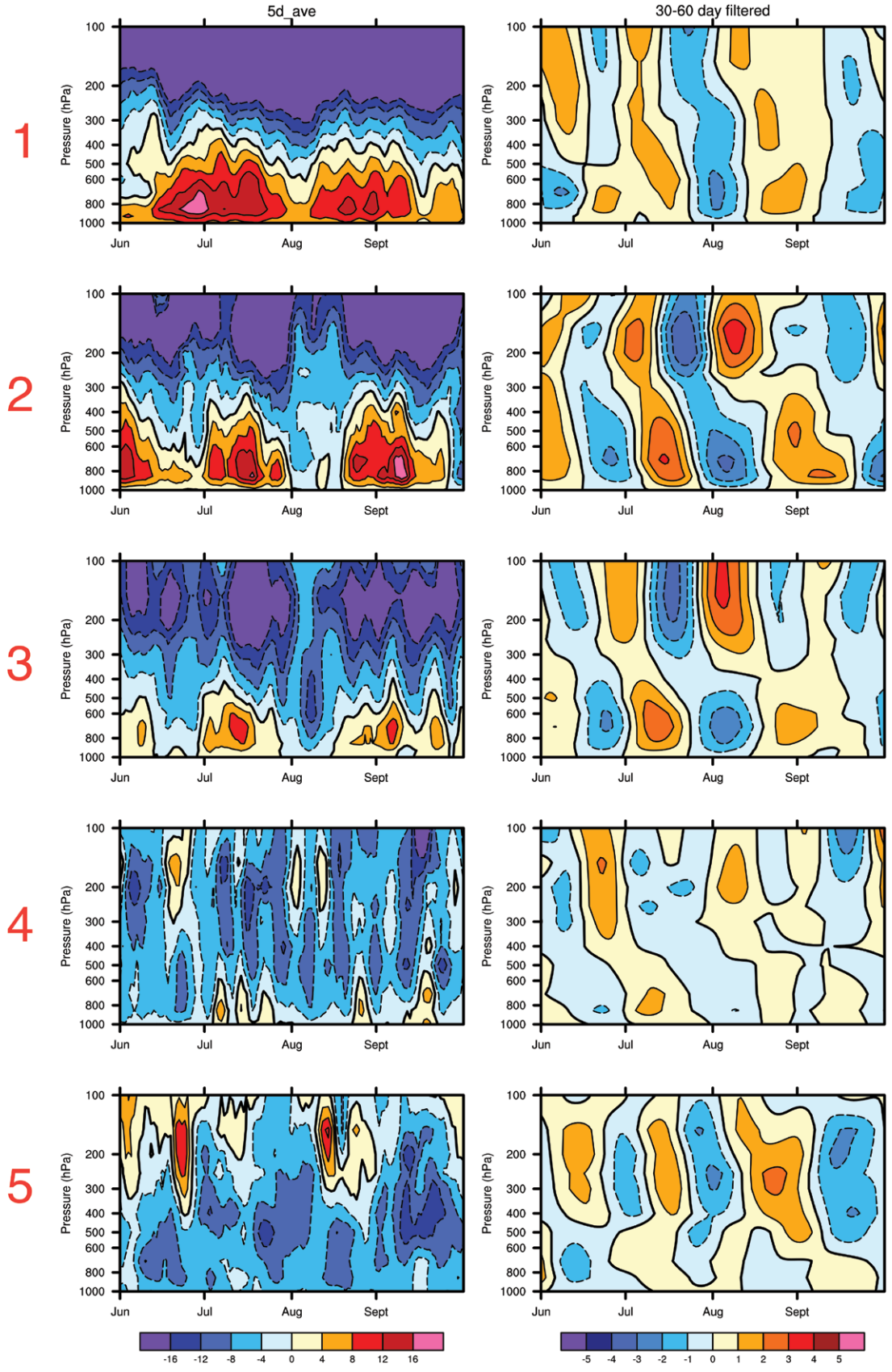

Fig. 7. (left) Vertical profiles of 5-day running mean zonal wind (m s^{-1}) from Jun to Sep 1958 and (right) corresponding 30–60-day filtered zonal wind fields at five stations (1–5; see Table 1 for details).

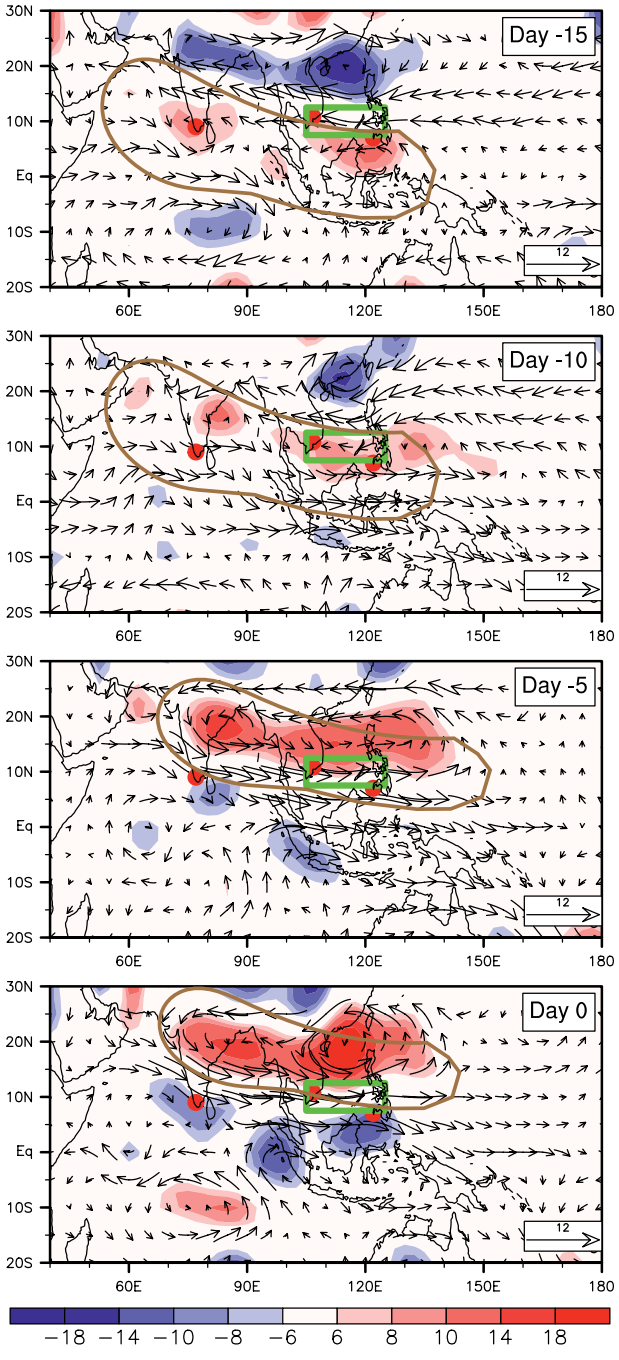

Fig. 8. Lagged regression patterns of 30–60-day filtered 700-hPa wind anomalies (vectors; m s^{-1}) and vorticity anomalies (shading; 10^{-6} s^{-1}) against 30–60-day filtered zonal wind anomalies averaged over the reference box (7.5°–12.5°N, 105°–125°E) (marked in green) for the period of Jun–Sep 1958–60. Brown curves are hand drawn to mark the anomalous large-scale cyclonic circulation.

easterly phases. This number is consistent with the finding by Liebmann et al. (1994) and confirms the assessment that TC activity in the western Pacific is modulated by the MJO.

An additional finding regarding TC activities in Xie63 is the preferred location of TC genesis. The original Fig. 3 in Xie63 is displayed in Fig. 10 with our enhancement. Xie63's Fig. 3 depicts the time variation of 700-hPa wind vectors observed at five stations spanning from south of India to the central Pacific. Xie63's assessment of this figure is that the TC genesis in the western Pacific is located mostly at the westerly–easterly confluence zone. The longitudinal distribution of the typhoon genesis locations is mostly between 120° and 150°E.

To verify Xie63's result on this, we examine the percentage of TC genesis that occurred over the westerly–easterly confluence zone, which is defined as a region where the absolute values of 700-hPa zonal wind are less than a given constant. Table 2 shows the percentage of TC genesis that occurred within 100°–160°E during 1 June–30 September of 1958–70 over the westerly–easterly confluence zone defined by different criteria. Seventy-five percent of the TC genesis appears over the westerly–easterly confluence zone, where the absolute zonal wind speed is less than 5 m s^{-1}. If a stricter criterion of 3 m s^{-1} is defined, then the percentage becomes 52%. From a dynamic point of view, energy accumulation (due to wave-scale contraction) over a confluence zone may accelerate the development of a TC-like vortex (Kuo et al. 2001).

In summary, the relationship between the zonal wind variability in Southeast Asia and typhoon genesis deduced by Xie63 has been confirmed with a longer (13 yr) dataset. This longer dataset reveals the following two results. First, typhoons occurred in the western Pacific mostly when Southeast Asia is experiencing strong westerlies, linking to the monsoon circulation. Second, typhoons occurred mostly in the region of a confluence zone where the monsoon westerly winds meet the trade easterlies.

SUMMARY AND CONCLUSIONS. The Madden–Julian oscillation (MJO) identified by Madden and Julian (1971, 1972) has been recognized as the most significant intraseasonal signal in the tropics, and its relationship with other weather–climate phenomena is broad and its impacts are far reaching. The original paper by Madden and Julian (1971) used the radiosonde data on Canton Island with Fourier analysis to reveal the outstanding signal of a 40–50-day oscillation. In their subsequent paper, Madden and Julian (1972) presented a more comprehensive picture of the intraseasonal signal globally using data from multiple stations. These pioneering studies have since brought tremendous attention within the atmospheric

sciences community to this phenomenon and stimulated substantial research efforts into the MJO that have advanced the understanding of tropical dynamics, its midlatitude impacts, and complex scale interactions.

It has come to our attention that an earlier study published in a Chinese journal (Xie et al. 1963) documented a similar oscillatory signal with a 1.5-month period using radiosonde data from three stations between 70° and 125°E in Southeast Asia. The investigation covered June–September for three years from 1958 to 1960. The 40–50-day signal found by Xie63 was strikingly strong as revealed by the variations of the 700-hPa zonal wind without any filtering. The original focus of Xie63 was on finding a possible relation between the Southeast Asian circulation and tropical cyclone (typhoon in the western Pacific) genesis. Xie63 identified that the occurrences of typhoons during these months are closely related to the variation of the low-level westerlies at these stations. Expanding the scope to the central Pacific, Xie63's analysis suggested that the western Pacific confluence zone (where the monsoon westerlies meet the trade easterlies) is the preferred zone of TC genesis.

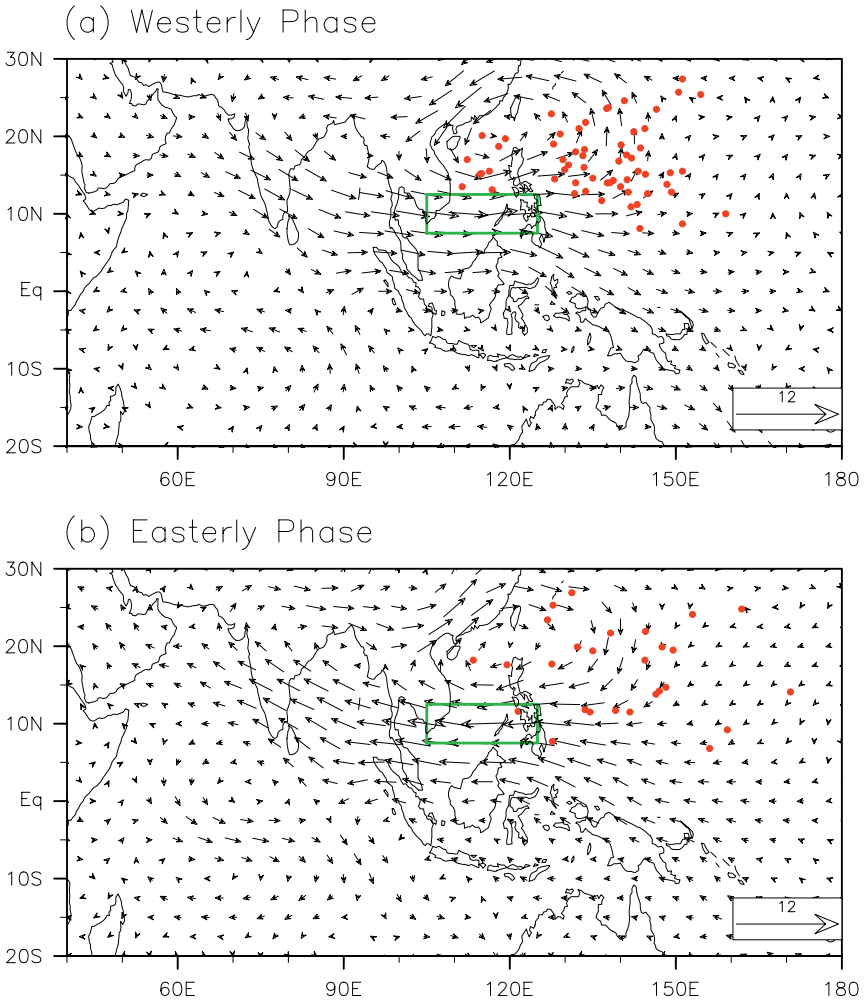

Fig. 9. Composite patterns of 30–60-day filtered anomalies in 700-hPa wind (vectors; m s^{-1}) and TC genesis location (dotted) for the MJO (a) westerly and (b) easterly phases during Jun–Sep 1958–70. The MJO westerly (easterly) phase is defined as occurring when the 30–60-day filtered 700-hPa zonal wind averaged over the reference box (7.5°–12.5°N, 105°–125°E) (marked in green) is greater (less) than positive (negative) one standard deviation.

Table 2. Percentages of the occurrence of TC numbers over the westerly–easterly confluence zone, which is based on the background 5-day running mean 700-hPa zonal wind speed averaged over 5°–15°N. The analysis period is Jun–Sep 1958–70.

Absolute zonal wind	TC number (%)
Less than 5 m s^{-1}	75
Less than 4 m s^{-1}	65
Less than 3 m s^{-1}	52

The purpose of this paper is to bring attention to the recognition of Xie63 pioneering discovery. To verify the results presented in Xie63, in which all of the analysis and figures were hand drawn based on a short data record, we first reproduced the original results using available radiosonde data at stations used by Xie63. The analysis was extended to a longer period from 1958 to 1970 so that it could cover the analysis periods of both Xie63 and MJ71 for better comparison of the strengths of the intraseasonal signals at Southeast Asia stations found by Xie63 and on Canton Island, as discovered by MJ71.

The 40–50-day oscillation identified by Xie63 using the unfiltered zonal wind dataset at several stations from the tropical Indian Ocean to the

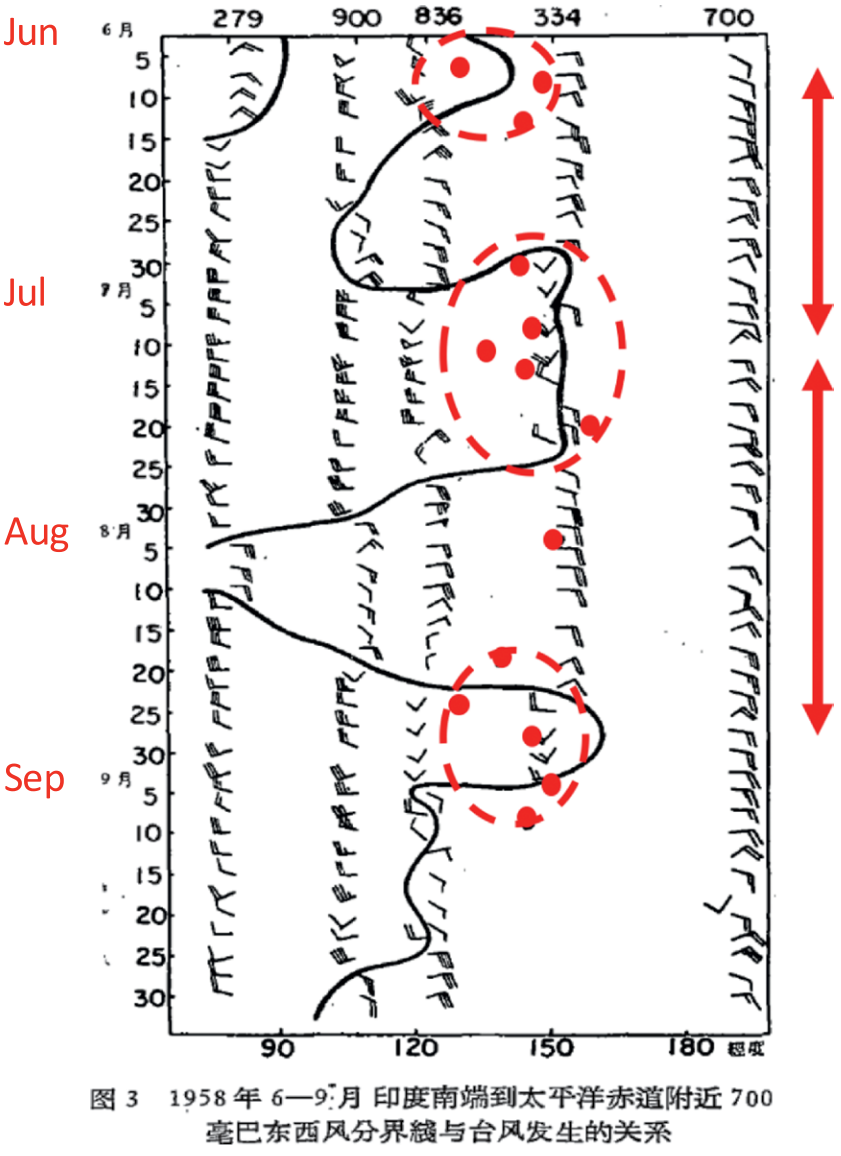

图 3　1958 年 6—9 月 印度南端到太平洋赤道附近 700 毫巴东西风分界綫与台风发生的关系

Fig. 10. Figure 3 from Xie63, which shows a time–longitude diagram of 700-hPa wind (wind barbs) and typhoon genesis locations (red dots, originally marked in black) during Jun–Sep 1958. The station numbers are listed at the top. Note that Xie63 used station 43279 (labeled as 279) instead of station 43371 in this figure, but their locations are very close (within 4° longitude apart). Circles highlight clusters of genesis events and arrows their periods, added by the authors of this current study.

western Pacific is confirmed to be robust from June to September. Compared to the Canton Island station (91701), the MJO variability over the Southeast Asian monsoon region is stronger, in both the lower and upper troposphere.

The relationship between the zonal wind variability in Southeast Asia and the typhoon genesis deduced by Xie63 is also confirmed using a larger data sample: 1) typhoons occur mostly when Southeast Asia is experiencing strong westerlies linked to the monsoon circulation and 2) typhoons occur mostly in the confluence region where the monsoon westerlies meet the easterly trade winds. For the 13 years (1958–70) of summers, 92% of typhoons occurred when station 48900 experienced westerlies. Meanwhile, 75% of WNP typhoons occurred in the westerly–easterly confluence zone defined as a region where the magnitude of the zonal flow at 700 hPa is less than 5 m s^{-1}.

The pioneering studies of Madden and Julian (1971, 1972) have been widely accepted as the discovery of the MJO. The identification of the 40–50-day periodicity contained in the Xie63 paper is nowhere near as meticulous, comprehensive, or rigorous as that done by Madden and Julian (1971, 1972). Xie63 did not do spectral analysis and qualitatively inferred a 40–50-day time scale from unfiltered wind fields over a relatively small number of events. Thus, the work by Madden and Julian (1971, 1972) remains a model of how spectral analysis should be used to identify a significant oscillation.

That said, the broader atmospheric research community should recognize the work by Xie et al. (1963) that phenomenologically identified the 40–50-day signal eight years earlier and its discovery of the relationship between MJO and TC genesis three decades earlier than studies on this subject published outside China. Since meteorology is a science that impacts people's lives globally and that is pursued by people everywhere, there must exist many other hidden gems that were published in earlier days in non-English journals that were unknown beyond their countries of origin. This current paper serves the purpose of bringing out one such gem to light and encourages others to do the same.

ACKNOWLEDGMENTS. This work was supported by China National Key R&D Program 2017 YFA0603802 and 2015CB453200; NSF AGS-16-43297; NSFC Projects 41630423, 41705059, 41475084, and 41575043; Jiangsu Projects BK20150062 and R2014SCT001; and the Priority Academic Program Development of Jiangsu Higher Education Institutions (PAPD). This is School of Ocean and Earth Science and Technology (SOEST) Contribution Number 10343, International Pacific Research Center (IPRC) Contribution Number 1317, and Earth System Modeling Center (ESMC) Contribution Number 207.

REFERENCES

Annamalai, H., and J. Slingo, 2001: Active/break cycles: Diagnosis of the intraseasonal variability of the Asian summer monsoon. *Climate Dyn.*, **18**, 85–102, https://doi.org/10.1007/s003820100161.

Cao, X., T. Li, M. Peng, W. Chen, and G. Chen, 2014: Effects of monsoon trough intraseasonal oscillation on tropical cyclogenesis over the western North Pacific. *J. Atmos. Sci.*, **71**, 4639–4660, https://doi.org/10.1175/JAS-D-13-0407.1.

Fu, X., B. Wang, T. Li, and J. P. McCreary, 2003: Coupling between northward-propagating intraseasonal oscillations and sea surface temperature in the Indian Ocean. *J. Atmos. Sci.*, **60**, 1733–1783, https://doi.org/10.1175/1520-0469(2003)060<1733:CBNIOA>2.0.CO;2.

Hartmann, D. L., and M. L. Michelsen, 1989: Intraseasonal periodicities in Indian rainfall. *J. Atmos. Sci.*, **46**, 2838–2862, https://doi.org/10.1175/1520-0469(1989)046<2838:IPIIR>2.0.CO;2.

——, and E. D. Maloney, 2001: The Madden–Julian oscillation, barotropic dynamics, and North Pacific tropical cyclone formation. Part II: Stochastic barotropic modeling. *J. Atmos. Sci.*, **58**, 2559–2570, https://doi.org/10.1175/1520-0469(2001)058<2559:TMJOBD>2.0.CO;2.

——, M. L. Michelsen, and S. Klein, 1992: Seasonal variations of tropical intraseasonal oscillations: A 20–25-day oscillation in the western Pacific. *J. Atmos. Sci.*, **49**, 1277–1289, https://doi.org/10.1175/1520-0469(1992)049<1277:SVOTIO>2.0.CO;2.

Hendon, H. H., and M. L. Salby, 1994: The life cycle of the Madden–Julian oscillation. *J. Atmos. Sci.*, **51**, 2225–2237, https://doi.org/10.1175/1520-0469(1994)051<2225:TLCOTM>2.0.CO;2.

Hsu, H. H., B. J. Hoskins, and F.-F. Jin, 1990: The 1985/86 intraseasonal oscillation and the role of the extratropics. *J. Atmos. Sci.*, **47**, 823–839, https://doi.org/10.1175/1520-0469(1990)047<0823:TIOATR>2.0.CO;2.

Hsu, P.-C., and T. Li, 2012: Role of the boundary layer moisture asymmetry in causing the eastward propagation of the Madden–Julian oscillation. *J. Climate*, **25**, 4914–4931, https://doi.org/10.1175/JCLI-D-11-00310.1.

——, ——, and C.-H. Tsou, 2011: Interactions between boreal summer intraseasonal oscillations and synoptic-scale disturbances over the western North Pacific. Part I: Energetics diagnosis. *J. Climate*, **24**, 927–941, https://doi.org/10.1175/2010JCLI3833.1.

Jiang, X., T. Li, and B. Wang, 2004: Structure and mechanisms of the northward propagating summer intraseasonal oscillation. *J. Climate*, **17**, 1022–1039, https://doi.org/10.1175/1520-0442(2004)017<1022:SAMOTN>2.0.CO;2.

——, and Coauthors, 2015: Vertical structure and physical processes of the Madden–Julian oscillation: Exploring key model physics in climate simulations. *J. Geophys. Res. Atmos.*, **120**, 4718–4748, https://doi.org/10.1002/2014JD022375.

Kalnay, E., and Coauthors, 1996: The NCEP/NCAR 40-Year Reanalysis Project. *Bull. Amer. Meteor. Soc.*, **77**, 437–471, https://doi.org/10.1175/1520-0477(1996)077<0437:TNYRP>2.0.CO;2.

Krishnamurti, T. N., 1985: Summer Monsoon Experiment: A review. *Mon. Wea. Rev.*, **113**, 1590–1626, https://doi.org/10.1175/1520-0493(1985)113<1590:SMER>2.0.CO;2.

——, and D. Subrahmanyam, 1982: The 30–50 day mode at 850 mb during MONEX. *J. Atmos. Sci.*, **39**, 2088–2095, https://doi.org/10.1175/1520-0469(1982)039<2088:TDMAMD>2.0.CO;2.

Kuo, H.-C., R. T. Williams, J.-H. Chen, and Y.-L. Chen, 2001: Topographic effects on barotropic vortex motion: No mean flow. *J. Atmos. Sci.*, **58**, 1310–1327, https://doi.org/10.1175/1520-0469(2001)058<1310:TEOBVM>2.0.CO;2.

Lau, K.-M., and P. H. Chan, 1986: Aspects of the 40–50 day oscillation during the northern summer as inferred from outgoing longwave radiation. *Mon. Wea. Rev.*, **114**, 1354–1367, https://doi.org/10.1175/1520-0493(1986)114<1354:AOTDOD>2.0.CO;2.

Li, T., 2014: Recent advance in understanding the dynamics of the Madden–Julian oscillation. *J. Meteor. Res.*, **28**, 1–33, https://doi.org/10.1007/s13351-014-3087-6.

——, and B. Wang, 2005: A review on the western North Pacific monsoon: Synoptic-to-interannual variabilities. *Terr. Atmos. Oceanic Sci.*, **16**, 285–314, https://doi.org/10.3319/TAO.2005.16.2.285(A).

——, F. Tam, X. Fu, T. Zhou, and W. Zhu, 2008: Causes of the intraseasonal SST variability in the tropical Indian Ocean. *Atmos. Oceanic Sci. Lett.*, **1**, 18–23.

——, C. Zhao, P.-C. Hsu, and T. Nasuno, 2015: MJO initiation processes over the tropical Indian Ocean during DYNAMO/CINDY2011. *J. Climate*, **28**, 2121–2135, https://doi.org/10.1175/JCLI-D-14-00328.1.

Liebmann, B., H. H. Hendeon, and J. D. Glick, 1994: The relationship between tropical cyclones of the western Pacific and the Indian Oceans and the Madden–Julian oscillation. *J. Meteor. Soc. Japan*, **72**, 401–411, https://doi.org/10.2151/jmsj1965.72.3_401.

Madden, R. A., 1986: Seasonal variations of the 40–50 day oscillation in the tropics. *J. Atmos. Sci.*, **43**, 3138–3158, https://doi.org/10.1175/1520-0469(1986)043<3138:SVOTDO>2.0.CO;2.

——, and P. R. Julian, 1971: Detection of a 40–50 day oscillation in the zonal wind in the tropical Pacific. *J. Atmos. Sci.*, **28**, 702–708, https://doi.org/10.1175/1520-0469(1971)028<0702:DOADOI>2.0.CO;2.

——, and ——, 1972: Description of global-scale circulation cells in the tropics with a 40–50 day period. *J. Atmos. Sci.*, **29**, 1109–1122, https://doi.org/10.1175/1520-0469(1972)029<1109:DOGSCC>2.0.CO;2.

Maloney, E., and D. L. Hartmann, 1998: Frictional moisture convergence in a composite life cycle of the Madden–Julian oscillation. *J. Climate*, **11**, 2387–2403, https://doi.org/10.1175/1520-0442(1998)011<2387:FMCIAC>2.0.CO;2.

——, and ——, 2000a: Modulation of eastern North Pacific hurricanes by the Madden–Julian oscillation. *J. Climate*, **13**, 1451–1460, https://doi.org/10.1175/1520-0442(2000)013<1451:MOENPH>2.0.CO;2.

——, and ——, 2000b: Modulation of hurricane activity in the Gulf of Mexico by the Madden–Julian oscillation. *Science*, **287**, 2002–2004, https://doi.org/10.1126/science.287.5460.2002.

——, and ——, 2001: The Madden–Julian oscillation, barotropic dynamics, and North Pacific tropical cyclone formation. Part I: Observations. *J. Atmos. Sci.*, **58**, 2545–2558, https://doi.org/10.1175/1520-0469(2001)058<2545:TMJOBD>2.0.CO;2.

Murakami, M., 1976: Analysis of summer monsoon fluctuations over India. *J. Meteor. Soc. Japan*, **54**, 15–31, https://doi.org/10.2151/jmsj1965.54.1_15.

Murakami, T., and T. Nakazawa, 1985: Tropical 45 day oscillations during the 1979 Northern Hemisphere summer. *J. Atmos. Sci.*, **42**, 1107–1122, https://doi.org/10.1175/1520-0469(1985)042<1107:TDODTN>2.0.CO;2.

Ramella Pralungo, L., L. Haimberger, A. Stickler, and S. Brönnimann, 2014: A global radiosonde and tracked balloon archive on 16 pressure levels (GRASP) back to 1905—Part 1: Merging and interpolation to 00:00 and 12:00 GMT. *Earth Syst. Sci. Data*, **6**, 185–200, https://doi.org/10.5194/essd-6-185-2014.

Sobel, A. H., and E. Maloney, 2013: Moisture modes and the eastward propagation of the MJO. *J. Atmos. Sci.*, **70**, 187–192, https://doi.org/10.1175/JAS-D-12-0189.1.

Vitart, F., 2014: Evolution of ECMWF sub-seasonal forecast skill score. *Quart. J. Roy. Meteor. Soc.*, **140**, 1889–1899, https://doi.org/10.1002/qj.2256.

Wang, B., and H. Rui, 1990: Synoptic climatology of transient tropical intraseasonal convection anomalies: 1975–1985. *Meteor. Atmos. Phys.*, **44**, 43–61, https://doi.org/10.1007/BF01026810.

——, and X. Xie, 1997: A model for the boreal summer intraseasonal oscillation. *J. Atmos. Sci.*, **54**, 72–86, https://doi.org/10.1175/1520-0469(1997)054<0072:AMFTBS>2.0.CO;2.

——, F. Liu, and G. Chen, 2016: A trio-interaction theory for Madden–Julian oscillation. *Geosci. Lett.*, **3**, 34, https://doi.org/10.1186/s40562-016-0066-z.

Wang, L., T. Li, E. Maloney, and B. Wang, 2017: Fundamental causes of propagating and nonpropagating MJOs in MJOTF/GASS models. *J. Climate*, **30**, 3743–3769, https://doi.org/10.1175/JCLI-D-16-0765.1.

Weickmann, K. M., 1983: Intraseasonal circulation and outgoing longwave radiation modes during Northern Hemisphere winter. *Mon. Wea. Rev.*, **111**, 1838–1858, https://doi.org/10.1175/1520-0493(1983)111<1838:ICAOLR>2.0.CO;2.

Xiang, B., M. Zhao, X. Jiang, S.-J. T. Li, X. Fu, and G. Vecchi, 2015: The 3–4-week MJO prediction skill in a GFDL coupled model. *J. Climate*, **28**, 5351–5364, https://doi.org/10.1175/JCLI-D-15-0102.1.

Xie, Y.-B., S.-J. Chen, I.-L. Zhang, and Y.-L. Hung, 1963: A preliminarily statistic and synoptic study about the basic currents over southeastern Asia and the initiation of typhoon (in Chinese). *Acta Meteor. Sin.*, **33**, 206–217.

Yasunari, T., 1979: Cloudiness fluctuations associated with the Northern Hemisphere summer monsoon. *J. Meteor. Soc. Japan*, **57**, 227–242, https://doi.org/10.2151/jmsj1965.57.3_227.

——, 1980: A quasi-stationary appearance of 30 to 40 day period in the cloudiness fluctuations during the summer monsoon over India. *J. Meteor. Soc. Japan*, **58**, 225–229, https://doi.org/10.2151/jmsj1965.58.3_225.

——, 1981: Structure of an Indian summer monsoon system with around 40-day period. *J. Meteor. Soc. Japan*, **59**, 336–354, https://doi.org/10.2151/jmsj1965.59.3_336.

Zhang, C., 2005: Madden–Julian oscillation. *Rev. Geophys.*, **43**, RG2003, https://doi.org/10.1029/2004RG000158.

——, 2013: Madden–Julian oscillation: Bridging weather and climate. *Bull. Amer. Meteor. Soc.*, **94**, 1849–1870, https://doi.org/10.1175/BAMS-D-12-00026.1.

——, and J. Ling, 2017: Barrier effect of the Indo-Pacific Maritime Continent on the MJO: Perspectives from tracking MJO precipitation. *J. Climate*, **30**, 3439–3459, https://doi.org/10.1175/JCLI-D-16-0614.1.

Zhao, C.-B., T. Li, and T. Zhou, 2013: Precursor signals and processes associated with MJO initiation over the tropical Indian Ocean. *J. Climate*, **26**, 291–307, https://doi.org/10.1175/JCLI-D-12-00113.1.

AMS Members

Give a great gift at a great price

Looking for the perfect present for the weather enthusiast in your life? Want to make a valuable contribution to your local library or community college?

Send a subscription to Weatherwise magazine for just $24.95*—That's nearly 50% off the list price!

Contact Member Services by e-mail at **amsmem@ametsoc.org** or by phone at **617-227-2425** to place all of your Weatherwise orders today!

Written for a general audience, Weatherwise offers a colorful and nontechnical look at recent discoveries in meteorology and climatology.

Check out the latest table of contents at www.weatherwise.org.

Want your own?
Then order a personal subscription at the same great price.

*Cost for delivery outside of the U.S. is $40.95. Weatherwise is available to AMS Members through a cooperative agreement with Taylor & Francis Group LLC, the publishers of Weatherwise.